NANO LETTERS

2003
Vol. 3, No. 2
139−142

Controlled Assembly of Conducting Monomers for Molecular Electronics

M. Hadi Zareie, Hong Ma, Bryan W. Reed, Alex K.-Y. Jen,* and Mehmet Sarikaya*

Materials Science & Engineering, University of Washington, Seattle, Washington 98195

Received October 5, 2002; Revised Manuscript Received December 2, 2002

ABSTRACT

We report controlled self-assemblies of two molecules as crystalline arrays on gold substrates at room temperature. The size, shape, orientation, and ordered assemblies of molecular wires can be engineered through a delicate interplay of the intermolecular π–π stacking and chemisorptive substrate–linker interactions. In particular, the molecule based on a fused aromatic, anthracene, forms an ordered 2D stacked array. Through scanning tunneling spectroscopy, we demonstrate changes in the electronic behavior of single molecules that form into superlattices. The ability to assemble predictable 2D crystals and understand the order-related electronic behavior of single molecular components could allow for the future design of nanopatterned arrays as a controlled platform toward further miniaturization of electronic devices.

The premise in molecular electronics is in building future nanodevices, the ultimate in miniaturization in computing, using individual molecules that can perform functions identical or analogous to those of the conductors, switches, diodes, transistors, and other key components of today's microcircuits.[1−3] In previous work, assemblies of molecules were used in concert mostly to operate as domains in devices, not yet reaching the miniaturization of a single molecule.[4−8] New ways to pattern millions of wires, each as a separate entity, are necessary in constructing transistors and other devices to realize complex circuitry.[1,3,9,10] We demonstrate such ordered patterns in this paper.

A single molecule is the smallest conceivable entity that could have the required complexity and be individually designed and manipulated for incorporation into electronic devices as an addressable smallest "bit" (e.g., read/write).[4,6,11−13] A molecular wire is a long, highly conjugated molecule in which a delocalized network of π-symmetry orbital provides a pathway for electron conduction.[14] These rigid molecules, containing various forms of aromatic (or phenyl) groups along their backbones, generally have a small energy gap, behaving like semiconductors. Using the well-established thiol chemistry, molecular wires have been assembled onto gold substrates using SH-functionalized ends as linkers.[14,15] If each molecule could act as a single device (as demonstrated in special cases), a large number ($>10^{15}$) of devices could potentially be assembled using routine chemistry approaches.[1−4] The task of addressing a large number of ordered molecular-scale devices is presently unattainable. However, ordering molecules of well-defined structures into predictable arrays and understanding their behavior would be a significant step in the robust design of nanoscale devices.[1−3]

Two ways of ordering molecules into arrays are nanolithography and self-assembly. Large-scale ordering has mostly been elusive by nanolithography mainly because of inefficiently slow processes and limitations of size control.[4,16−18] The process of ordering of self-assembled monolayers in which thiolated molecules (alkanethiols) tightly bind and form well-ordered arrays conforming onto a Au(111) surface,[1−5,19,20] however, has matured during the past decade. Thiol linkers could also be used for assembling molecules with rigid aromatic backbones. Aromatic thiolates, assembled this way, have been used as molecular wires, but their study has been mostly limited to simple molecules such as the derivatives of diphenyl acetylene.[5−10] The basis of ordering of aromatic thiolates would be different than those of alkanethiols. In the latter, strong S−Au(111) bonding is the main driving force, as the alkanes are axially symmetric; in the former, because of a large surface area, intermolecular (lateral) interactions among the aromatic conjugated moieties may play a major role. Here we present the results of two aromatic thiolates that conform into ordered assemblies and describe their electronic properties on the basis of the differences in molecular architecture. Furthermore, we show that, depending on short and long-range order, individual molecules display significantly different electronic properties (measured by scanning tunneling spectroscopy, STS).

Although many conjugated molecules can be used as molecular wires, phenylacetylene compounds appear to be promising; they are stable in air and against UV light, have a rigid framework resisting conformational instability, and

* Corresponding authors. E-mail: ajen@u.washington.edu and sarikaya@u.washington.edu.

10.1021/nl025833x CCC: $25.00
Published on Web 01/17/2003

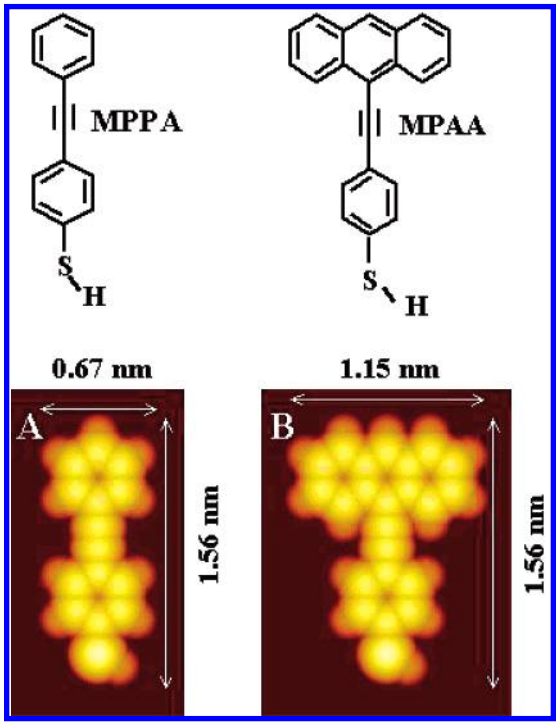

Figure 1. Schematic illustration of the molecular conductors: (A) MPPA and (B) MPAA and their corresponding van der Waals structures. The two molecular wires, MPAA and MPPA, were prepared through the Sonogashira coupling[23] of 4-iodophenylthioester with phenylacetylene and 9-anthrylacetylene, respectively. Gold films (50−100 nm thick) were prepared by the slow vapor deposition of high-purity gold onto freshly cleaved mica followed by annealing at 425 °C for 24 h in vacuum. Gold films were cut into sections, washed with ethanol, and dried under a stream of high-purity argon immediately before use. The STM scans of Au(111) films showed atomically flat surfaces of a few square millimeter grains with step edges clearly visible. The gold substrates were immersed in 60 μM ethanol solution of either of the molecules for 12 to 24 or 48 h and longer, followed by rinsing with ethanol and drying with nitrogen gas before STM observations.

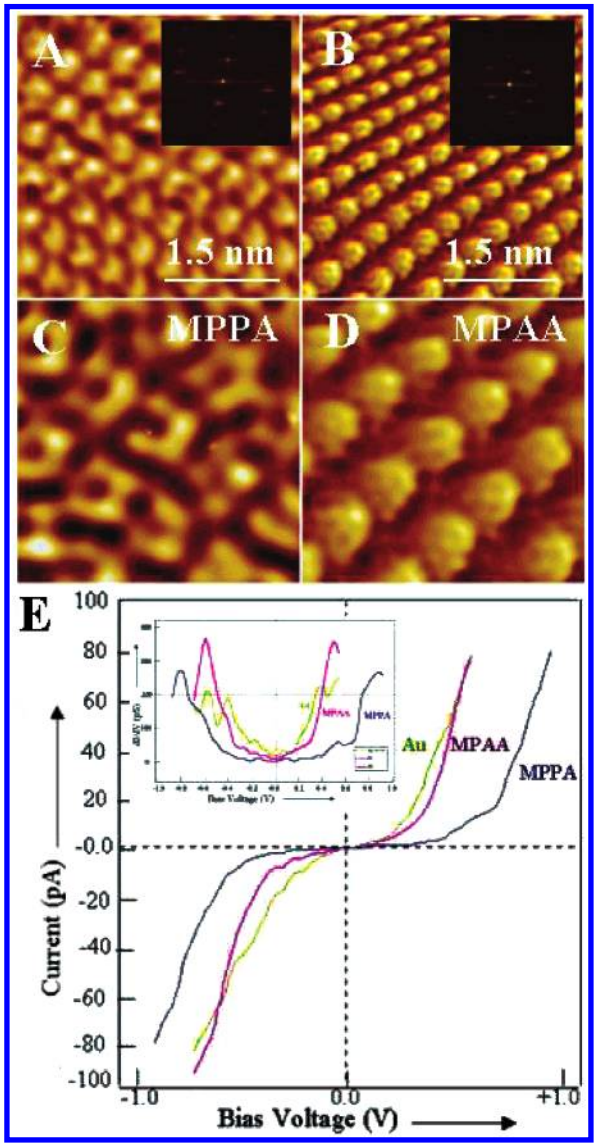

Figure 2. STM images of ordered assemblies of MPPA (A and C) and MPAA (B and D). Samples were prepared by dipping into 60 μM solution for 24 h. The STM images were recorded under constant-current mode with a 2−10 pA tunneling current and a −200 to −400 mV bias voltage. Both the high-resolution images and their Fourier transforms were used for the determination of structural parameters. (E) Current−voltage characteristics of the individual molecules in MPPA and MPAA compared to that from a bare Au surface. The inset shows dI/dV characteristics of the molecules and of a Au substrate on mica. STM and STS measurements were performed using either a Nanoscope-III or a Nanosurf EasyScan system operated in air at room temperature. Freshly cut Pt−Ir tips (0.2 mm) were used, and STM images were obtained with typical tip−sample bias voltages of up to −200 to −400 mV and tunneling currents of ∼2 to 10 pA.

can be attached to gold strongly (40 kcal/mol) via thiol-terminated ends. We used two conjugated molecules (4-mercaptophenyl)-phenylacetylene **(**MPPA**)** and (4-mercaptophenyl)anthrylacetylene **(**MPAA**)**; the former is a fairly well-known molecule,[4,5,11] and the latter is a new design (Figure 1). In addition to possessing the desired wiring properties, the introduction of aromatic fused rings into the newly designed anthrylacetylene molecule, MPAA, is expected to lead to a delicate interplay of the strong $\pi-\pi$ intermolecular stacking and chemisorptive gold−-thiol interactions, thereby generating nanopatterns with different features compared to those of simple phenylacetylene molecules such as MPPA.

The gold-coated substrates were removed from dilute solutions containing MPPA and MPAA at different time intervals as soon as ordered assemblies of the molecules were ensured. The STM images of both MPPA and MPAA (Figure 2, after 24 h) reveal oblique lattices with different unit cell structures, although the shapes of the individual molecules are not fully discernible possibly because of tip convolution. The real-space unit cell lattice parameters (Figure 4) $a \times b$ and θ are 0.97 × 1.05 ± 0.1 nm, 46 ± 2° and 0.90 × 1.00 ± 0.1 nm, 74 ± 2° for MPPA and MPAA, respectively. Because of the significantly different molecular architecture (one versus three fused phenyl units), different unit cell structures could be expected, but the differences in the detailed unit cells could not be predicted. Assuming an atomically flat Au(111) surface without reconstruction, these values of the unit cells correspond to $\sqrt{13}\bar{a} \times 3\bar{a}$, 46° and $\sqrt{13}\bar{a} \times 3\bar{a}$, 74° ($\bar{a} = \bar{a}_{(111)} = 0.288$ nm) superstructures for MPPA and MPAA, respectively, with an area ratio of $^3/_4$.

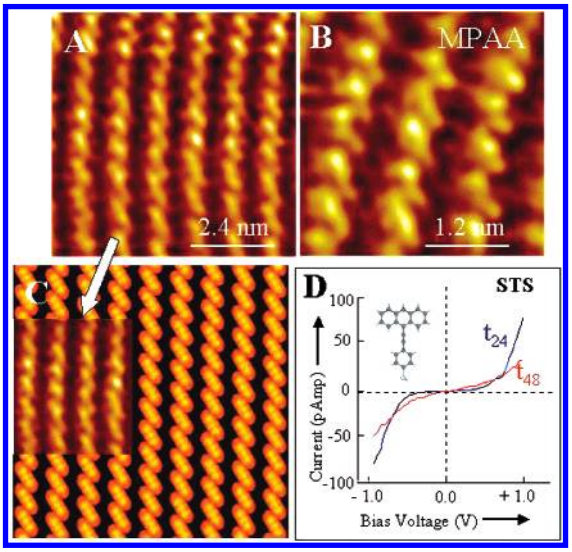

Figure 3. STM images (A and B) are from the new crystalline assembly of the MPAA molecules after soaking gold substrates in solution beyond 48 h (imaging conditions are the same as in Figure 2). (C) Modeling of the real-space structure of MPAA based on the van der Waals structure and the parameters obtained in A. The experimental image in the inset matches the model. (D) *I*/*V* characteristics of an isolated MPAA molecule after 48 h of ordering (red) compared to that after 24 h of assembly (black). The smooth change in polarity in *I*/*V* behavior as well as the narrow gap in d*I*/d*V* are indications of ordering effects on the electronic properties of the same MPAA molecule.

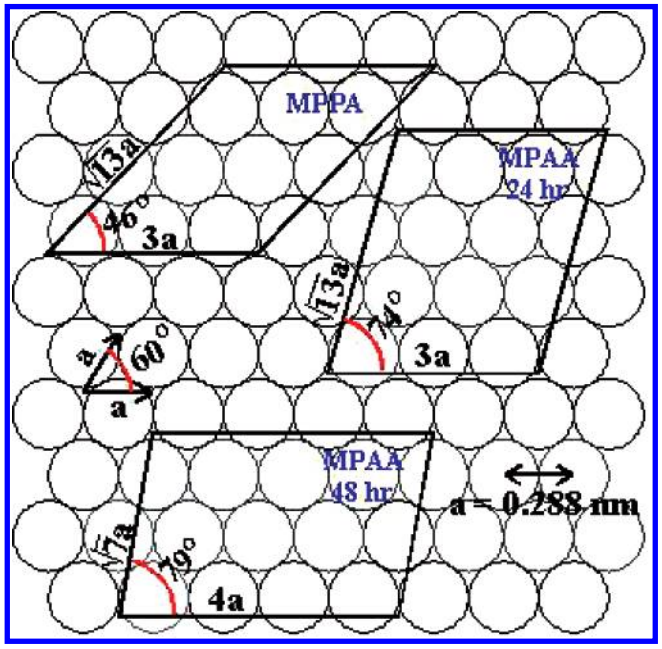

Figure 4. Schematic real-space adsorbate unit cells of MPPA and MPAA after 24 h of assembly and of MPAA after 48 h of assembly as conformed on the Au(111) lattice. All unit cells are commensurate with the underlying gold lattice but with different lattice parameters. Instead the $\sqrt{3}\bar{a} \times \sqrt{3}\bar{a}$ convention commonly used for alkanethiols, we used a convention that is simply based on an unreconstructed Au(111) surface, with a base of $\bar{a}_{(110)} \times \bar{a}_{(101)}$ and $\alpha = 60°$.

We also studied the dynamics of the assembly of the molecules. Although the assembled MPPA pattern was stable (beyond 24 h), MPAA organization has slowly changed and settled into a stable organization after 48 h (Figure 3) (staying stable even after an extended period of time, beyond 3 weeks). Quantitative analysis of the structure produced a new unit cell organization with lattice parameters of $0.85 \times 1.25 \pm 0.05$ nm and $78 \pm 2°$ corresponding to a $\sqrt{7}\bar{a} \times 4\bar{a}$ superstructure on the Au(111) surface (Figure 4). An inspection of the high-resolution STM images shows individual elongated entities corresponding to MPAA molecules with nearly head-on projection. The model of the quantitative structure (Figure 3c) reveals that, instead of end-to-end order, the molecules are stacked along a line with overlapping phenyl groups. This result may have significant implications in terms of the structure and long-term stability of aromatic thiolates that contain fused phenyl headgroups (MPAA) instead of single phenyl species (MPPA). Although both unit cells of the short- and long-time-ordered structures have the same area (12 Au atoms/cell, Figure 4), their short-range conformational structures are clearly different. The unique conformation may arise from a delicate interplay between the intermolecular interactions dominated by the anthryl groups, involving both steric hindrance and weak dipole−dipole interactions, and the strong S bond onto gold, where the latter appears to play a secondary role. The surface lattice initially formed by the MPPA is presumably close to the equilibrium (saturation) density, but the intermolecular distances are too large to form $\pi-\pi$ stacking (and no amount of uniform tilting or rotation of the molecules can overcome this distance). But if two molecules are separated by a distance of $\sqrt{7}\bar{a}$, then a rotation of 30° (consistent with the images), followed by a tilt of 12°, will cause the ends of the anthracene groups to overlap in a manner very similar to the interplanar stacking of graphite, with an interplanar spacing of 0.37 nm (compared to 0.34 nm for graphite). By changing to the $\sqrt{7}\bar{a} \times 4\bar{a}$ unit cell, the molecules can achieve this graphitelike configuration without changing their surface density.

The current−voltage (*I*/*V*) characteristics of the individual molecules were measured and correlated with their conformational structures in the long-range-ordered arrays. The *I*/*V* curves (Figure 2 e) for MPPA and MPAA both show semiconducting behavior compared to that from a bare surface of Au (metallic). On the basis of the d*I*/d*V* characteristic, these molecules have an average energy gap of 1.0 and 2.0 ± 0.2 eV, respectively (i.e., they are small band-gap semiconductors). More surprising is the molecular *I*/*V* characteristics of MPAA in two different conformational structures. The long-range-ordered wirelike structure (Figure 3d) appears to have improved conductivity and to have lowered the energy gap (1 eV).

The improved conductivity in the highly packed structure and the alteration of the energy gap may have originated from two possible effects. The first is due to a $\pi-\pi$ stacking interaction that would alter the energetics of the system, providing a driving force for the rearrangement of the molecules, causing changes in the band gap. The magnitude of the effect will depend on the overlap integral between the π orbitals on the adjacent molecules (i.e., it depends on the ability of these π electrons to tunnel between molecules).

The intermolecular interaction will spread to discrete energy states of the π orbitals, which one would get with isolated molecules, into bands. The bands would essentially be 1D, dominated by the overlap integrals among neighboring molecules all in the same π-stacked row with essentially no tunneling probability between rows. If the discrete states are spread out into a band, then one would expect the band gap to decrease by an amount comparable to the off-diagonal terms of the interaction Hamiltonian (i.e., the overlap integral between the π orbitals of the adjacent molecules).

The second effect would originate from the modification of the Au(111) surface electronic states by the presence of the monolayer. It is already known that in alkanethiols the regular spacing of the sulfur binding sites on the Au(111) lattice creates a surface superlattice due to reconstruction.[14,21] In the case of aromatic thiolates, one would expect superlattices with different lattice vectors to modify the gold-surface electronic states in different ways. Since electons moving from the organic molecule to the gold via the sulfur have to go through the gold surface, one would expect to get a modification of the tunneling amplitude due to the local electronic density of states at the surface being slightly different from that of the bulk. Since the SAMs represent a periodic modulation of the surface boundary condition, the different spatial symmetries of the two SAM structures would have a different effect on the energy-dependent LDOS at the Au surface.

The relative sizes of these two effects might be compared by considering the relative probabilities of the tunneling directly between two molecules via $\pi-\pi$ stacked overlap regions and of tunneling through a C−S−Au linkage into the next molecule. Between the two, the latter effect might be more difficult to calculate. It should be indicated that the band-gap reduction may also be explained in the same way as to the longer-wavelength emission from aggregated polymers and the associated improvements in conductivity.[22]

In summary, our results show that the short- and long-range order and long-term stability of the aromatic thiolate assemblies are dependent on their molecular architecture and the intermolecular forces. More importantly, the electronic properties of an individual molecule in an ensemble do not depend only on its molecular structure (e.g., number of phenyls), the length of the acetylene backbone, and the nature of the substrate/molecule binding but also very much on the local ordering of the molecules. The local ordering of the assembled molecules changes the intermolecular interactions and therefore the molecular orbital overlap, possibly affecting surface states on the gold substrate that lead to new electron paths for conduction. This provides another tool in the control of the nanoscale architecture of molecular electronics and would also be applicable in harvesting other nanoscale phenomena such as nanophotonics and nanomagnetics.

Acknowledgment. This research was supported by ARO-DURINT (DAAD19-01-04999) and US-AFOSR programs.

References

(1) Aviram, A.; Ratner, M. A. *Chem. Phys. Lett.* **1974**, *29*, 277.
(2) Metzger, R. M. *Acc. Chem. Res.* **1999**, *32*, 950.
(3) Collier, C. P.; Mattersteig, G.; Wong, E. W.; Luo, Y.; Beverly, K.; Sampaio, J.; Raymo, F. M.; Stoddart, J. F.; Heath, J. R. *Science (Washington, D.C.)* **2000**, *289*, 1172.
(4) Chen, J.; Reed, M. A.; Rawlett, A. M.; Tour, J. M. *Science (Washington, D.C.)* **1999**, *286*, 1550.
(5) Leatherman, G.; Durantini, E. N.; Gust, D.; Moore, T. A.; Moore, A. L.; Stone, S.; Zhou, Z.; Rez, P.; Liu, Y. Z.; Lindsay, S. M. *J. Phys. Chem. B* **1999**, *103*, 4010.
(6) Huang, Y.; Duan, X.; Cui, Y.; Lauhon, L. J.; Kim, K.-H.; Lieber, C. M. *Science (Washington, D.C.)* **2001**, *294*, 1313.
(7) Schön, J. H.; Meng, H.; Bao, Z. N. *Nature (London)* **2001**, *413*, 2138.
(8) Cui, X. D.; Primak, A.; Zarate, X.; Tomfohr, J.; Sankey, O. F.; Moore, A. L.; Moore, T. A.; Gust, D, Harris, G.; Lindsay, S. M. *Science (Washington, D.C.)* **2001**, *294*, 571.
(9) Bachtold, A.; Hadley, P.; Nakanishi, T.; Dekker: C. *Science (Washington, D.C.)* **2001**, *294*, 1317.
(10) Derycke, V.; Martel, R.; Appenzeller, J.; Avouris, Ph. *Nano Lett.* **2001**, *1*, 453.
(11) Bumm, L. A.; Arnold, J. J.; Cygan, M. T.; Dunbar, T. D.; Burgin, T. P.; Jones, L., II; Allara, D. L.; Tour, J. M.; Weiss, P. S. *Science (Washington, D.C.)* **1996**, *271*, 1705.
(12) Donhauser, Z. J.; Mantooth, B. A.; Kelly, K. F.; Bumm, L. A.; Monnell, J. D.; Stapleton, J. J.; Price, D. W., Jr.; Rawlett, A. M.; Allara, D. L.; Tour, J. M.; Weiss, P. S. *Science (Washington, D.C.)* **2001**, *292*, 2303.
(13) Tour, J. M.; Rawlett, A. M.; Kozaki, M.; Yao, Y.; Jagessar, R. C.; Dirk, S. M.; Price, D. W.; Reed, M. A.; Zhou, C.-W.; Chen, J.; Wang, W.; Campbell, I. *Chem.—Eur. J.* **2001**, *7*, 5118.
(14) Fuxen, C.; Aazzam, W.; Arnold, R.; Witte, G.; Terfort, A.; Woll, C. *Langmuir* **2001**, *17*, 3689.
(15) Gittins, D. I.; Bethell, D.; Schiffrin, D. J.; Nichols, R. J. *Nature (London)* **2000**, *408*, 67.
(16) Chen, J.; Reed, M. A.; Asplund, C. L.; Cassell, A. M.; Myrick, M. L.; Rawlett, A. M.; Tour, J. M.; Van Patten, P. G. *Appl. Phys. Lett.* **1999**, *75*, 624.
(17) Gimzewski, J. K.; Joachim, C. *Science (Washington, D.C.)* **1999**, *283*, 1683.
(18) Fan, F. F.; Yang, J.; Dirk, S. M.; Price, D. W.; Kosynkin, D.; Tour, J. M.; Bard, A. J. *J. Am. Chem. Soc.* **2001**, *123*, 2454.
(19) Dhirani, A.-A.; Zehner, R. W.; Hsung, R. P.; Guyot-Sionnest, P.; Sita, L. R. *J. Am. Chem. Soc.* **1996**, *118*, 3319.
(20) Ishida, T.; Mizutani, W.; Azehara, H.; Sato, F.; Choi, N.; Akiba, U.; Fujihira, M.; Tokumoto, H. *Langmuir* **2001**, *17*, 7459.
(21) Camillone, N., III; Chidsey, C. E. D.; Liu, G.; Scoles, G. *J. Am. Chem. Soc.* **1993**, *98*, 3503.
(22) Blatchford, J. W.; Jessen, S. W.; Lin, L. B.; Gustafson, T. L.; Fu, D. K.; Wang, H. L.; Swager, T. M.; MacDiarmid, A. G.; Epstein, A. J. *Phys. Rev. B* **1996**, *54*, 9180.
(23) Sonogashira, K.; Tohda, Y.; Shagihara N. *Tetrahedron Lett.* **1975**, *45*, 4467.

NL025833X